

Assessment of a multi-core optical fibre interferometer for strain sensing in aerospace structures

Oskar ARRIZABALAGA,^{1,*} Joel VILLATORO,^{1,2} Gaizka DURANA,¹ Iker GARCIA,¹
Ander MONTERO,³ Enrique. ANTONIO-LOPEZ,⁴ Axel. SCHLÜZGEN,⁴ Rodrigo
AMEZCUA-CORREA,⁴ Joseba ZUBIA,¹ Idurre SAEZ DE OCARIZ³

¹Department of Communications Engineering, Faculty of Engineering, University of the Basque Country (UPV/EHU), Alda. Urquijo s/n, E-48013 Bilbao, Spain

²IKERBASQUE—Basque Foundation for Science, E-48011 Bilbao, Spain

³Fundación Centro de Tecnologías Aeronáuticas (CTA), Miñano, Spain

⁴CREOL, The College of Optics & Photonics, University of Central Florida,
P.O. Box 162700, Orlando, Florida 32816-2700, USA

*Corresponding author: oskar.arrizabalaga@ehu.eus

Key words: multi-core, fibre interferometer, strain sensing.

Abstract

An optical fibre-based interferometric sensor consisting of a combination of single-mode fibre and multi-core fibre is used for strain sensing of aerospace structures. The optical sensor has been tested on a Carbon Fibre Reinforced Polymer specimen and compared with tested reference technologies as Fibre Bragg Gratings (FBGs) and strain gauges. The results are promising and the sensor performance compares with that of FBGs.

1 INTRODUCTION

Structural health monitoring (SHM) represents one of the major concerns for aeronautical structures and aircraft maintenance. As a matter of fact, the progressive ageing of an aircraft or aeronautical structure can compromise its durability and profitability, as well as the real effectiveness of conventional preventive maintenance philosophy, based on non-destructive techniques. The latter requires the integration of a network of sensors, actuators and detection algorithms synergistically coupled to continuum mechanics, fracture mechanics and damage mechanics. Therefore, destructive testing is not desirable.

In the last decade, sensors based on fibre Bragg grating (FBGs) have been widely used to sense strain in composite materials [1]. Due to their adaptable shape and small size, fibre optic sensors can be embedded easily into Carbon Fibre Reinforced Polymer (CFRP) composites, a material commonly used in aeronautical structures. Embedded fibre optic sensors do not affect the mechanical properties of host structures [2]. An additional advantage of fibre optic sensors is their immunity to electromagnetic fields and their multiplexing capabilities [3]. This has led to manufacturing techniques where the structures themselves have sensing capabilities which make them smart.

Despite their several advantages, the FBG-based sensors are not suitable for sensing in hostile environments such as those with high temperatures. The modulation of a standard FBG decays until it is completely depleted around 600°C [4]. FBGs which can resist high temperatures represent an important field of current research [5, 6]. However, FBG strain sensors for extreme temperatures have not been reported so far.



Nowadays, multi-core fibres (MCFs) are emerging as an alternative to devise sensors for strain and other physical parameters. In recent works [7, 8] it has been presented a new concept of interferometric device using multi-core fibres with excellent performance, which makes them—multi-core fibres—very appealing for strain sensing. One important advantage of multi-core fibres is their inherent resistivity to extreme temperatures up to 1000 °C.

In the following sections, we present and discuss a multi-core fibre-based interferometer which is proposed as a strain sensor to be used in an aerospace structure. First, the fabrication and principle of operation of the interferometer are described. The details of the specimen and the different surface-bonded sensors installed on it, both optical and electrical, are then presented. Afterwards, some preliminary results are shown and discussed. In those experimental results, the performance of the interferometer is compared with that of commercial sensors based on FBGs and strain gauges. Finally, the main conclusions of the work are drawn.

2 EXPERIMENTAL DETAILS

2.1 Sensor design and principle of operation

Our device consists in a SMF-MCF-SMF structure which is fabricated by a standard fusion splicing technique. A few centimeters of MCF is inserted between two segments of SMFs (see close-up in Figure 1). In our device, the cleaved end face of the second SMF acts as a mirror due to Fresnel reflection. The MCF used in our experiment was fabricated using the well-established stack and draw method. It consists of seven strongly coupled germanium-doped cores. Each core has a diameter of 11 μm , and a numerical aperture (NA) of 0.132. The core to core separation is 11 μm and the MCF diameter is 130 μm . It is important to mention here that the NA of the MCF matches that of a standard SMF (NA=0.14). This fact, combined with the similar dimensions of both types of fibres, makes the splicing simple and reproducible.

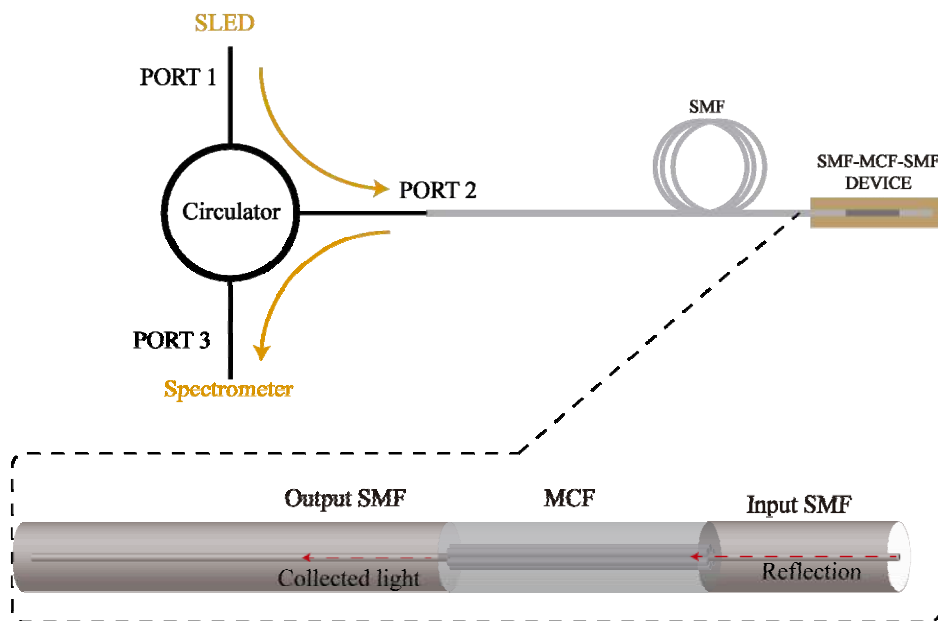


Figure 1: Schematic diagram of the MCF interferometer for strain sensing. Close-up: detail of the SMF-MCF-SMF structure.

The operating principle of the interferometer is simple. Owing to the circular symmetry of the MCF, only two super-modes are excited in the MCF by the fundamental mode of the SMF [9]. The supermodes interfere with each other which results in a periodic coupling of power between the centre and outer cores as the light propagates down the MCF. Spectrally, the interference generates a periodic transmission spectrum of the interferometer device. This is due to difference in propagation constants ($\Delta\beta$) of the super-modes. The wavelength dependence of $\Delta\beta$ causes the MCF to act like a directional coupler. Therefore, as the difference in propagation constants varies with wavelength, the power distribution across the cores at the facet of the output SMF will vary periodically in the spectrum domain and consequently the amount of light collected by the second SMF will vary accordingly [8, 9].

Axial strain applied to the MCF interferometer induces a small change in length of the MCF which results in a change of the propagation constants of the interfering modes. As a consequence of that, the interference pattern shifts. Therefore, by monitoring the wavelength shift, the axial strain can be obtained quantitatively by proper calibration of the optical interferometer built into the MCF. Figure 2 shows the spectra obtained for different strain levels applied to the specimen. The top figure shows how the spectra shift to shorter wavelengths when the axial strain increases, whereas the bottom graph shows the opposite behavior when the strain is decreased until completely removed. As a reference to determine the wavelength shift, the displacement of the higher peak in the interference pattern with applied strain has been considered.

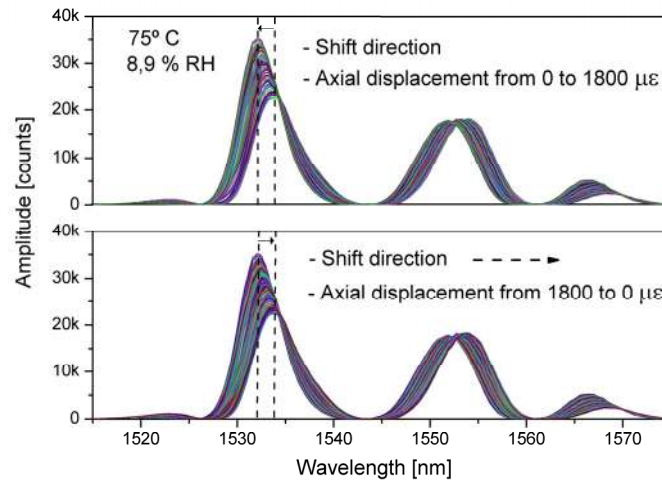


Figure 2: Top figure: interference pattern shift to shorter wavelengths when the strain applied to the specimen increases. Bottom figure: the spectrum recovers the initial position when the strain on the specimen is completely removed. The vertical dashed line represents, for each applied strain, the position of the highest peak in the interference pattern.

2.2 Preparation and installation of the MCF sensor

The MCF interferometer was assessed to sense strain in a specimen made of Carbon Fibre Reinforced Polymer (CFRP) with dimensions 0.41 m \times 0.19 m \times 0.05 m. On one side of the specimen two interferometers, each 9 cm in length, were bonded using epoxy resin. Also on the same side, a strain gauge and two FBGs were bonded as reference sensors to evaluate the performance of the MCF interferometer (see Figure 3(a)). The experiments were carried out in a certified aerospace test facility. The specimen was subjected to axial strain by means of a

hydraulic actuator, as shown in Figure 3(b). The experimental setup is similar to those frequently used in typical certification tests of aircraft structures, in which the load-application velocity is not considered.

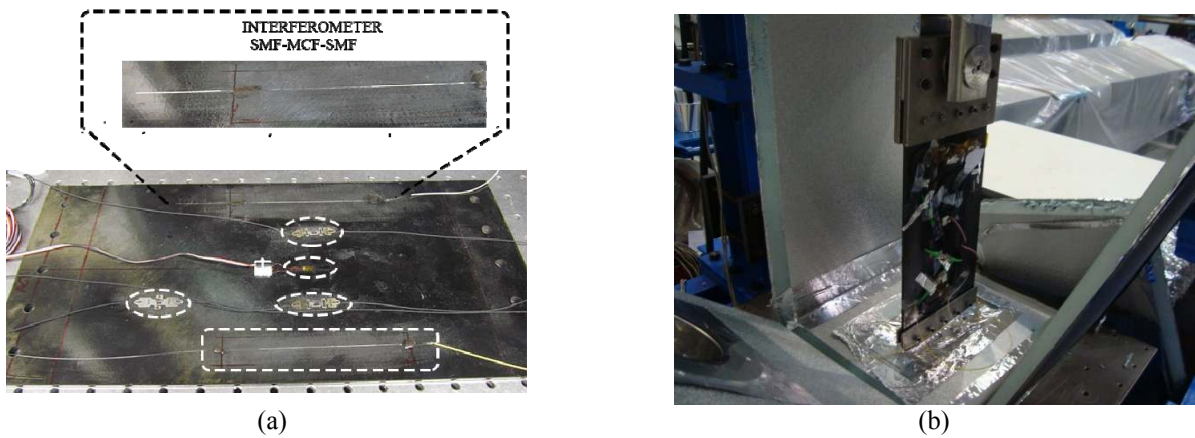


Figure 3: Photographs of the CFRP specimen with the different sensors installed on top of it. (a) The dashed rectangle highlights the MCF interferometers, and the dashed ellipses the strain gauge and FBGs. (b) Specimen mounted on the hydraulic system for traction tests.

3 RESULTS AND DISCUSSION

Figure 4 shows the linear behaviour of the sensor with applied strain. The black squares represent measured data when the axial strain increases from 0 to 1600 $\mu\epsilon$ in steps of 105 $\mu\epsilon$, whereas the red circles represent data when the axial strain decreases from the maximum strain value back to 0. As it can be observed from the figure, no hysteresis is appreciated when a complete strain cycle is applied to the specimen. Although not shown in Figure 4, the best linear fit has a Pearson’s correlation coefficient of 0.9986.

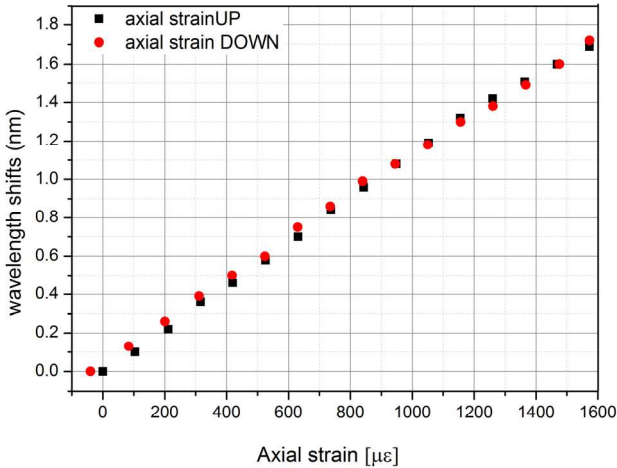


Figure 4: Wavelength shift of the highest peak in the interference pattern as a function of applied axial strain, both when the axis strain increases (black squares) and decreases (red circles). Position of highest peak when no axial strain is applied: $\lambda = 1533.8$ nm.

In the same axial strain range, the aerospace specimen was also subjected to a sinusoidal-like axial strain curve. Figure 5 shows the results obtained for the MCF sensor and its references.

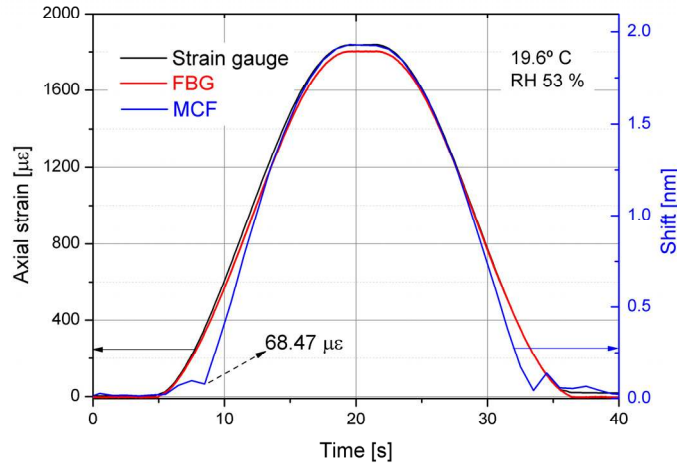


Figure 5: Comparative of our sensing device response with FBGs and strain gauge. The left ordinates axis shows the values measured by FBGs and strain gauge during the sinusoidal axial strain. Additionally, the right ordinates axis shows how many changes the interferometer spectrum in the same cycle. The length of time (abscissas axis) was arbitrarily chosen.

The left ordinates axis, refers to the strain strain subjected to the specimen measured by the FBGs and strain gauges whereas the right ordinate is for the wavelength shift of the higher peak of the spectrum obtained from the MCF interferometer.

Notice that our interferometer starts to detect the axial strain at the same time as the sensors, but its behaviour is not linear until $68.47 \mu\epsilon$ have been applied to the specimen. This might have occurred due to the installation a faulty of the MCF on the specimen; most probably, the SMF-MCF-SMF structure was not stretched taut during the bonding process.

4 CONCLUSIONS

Considering the shown preliminary results, it is demonstrated that MCF interferometers may be fabricated for sensitive strain sensing in an easy and fast way. Besides that, the fabrication process and final SMF-PCF-SMF structure is highly reproducible. Additionally, the performance of the sensor has been tested on an aeronautical specimen with the result of a performance similar to well established technologies in the aeronautical industry (FBGs and strain gauges).

ACKNOWLEDGEMENTS

This work has been funded in part by the Fondo Europeo de Desarrollo Regional (FEDER); by the Ministerio de Economía y Competitividad under project TEC2015-638263-C03-1-R; by the Gobierno Vasco/Eusko Jaurlaritza under projects IT933-16 and ELKARTEK; and by the University of the Basque Country UPV/EHU under programmes UFI11/16 and Euskampus.

REFERENCES

- [1] J. A. Güemes, J. M. Menendez, M. Frövel, I. Fernandez and J. M. Pintado, Experimental analysis of buckling in aircraft panels by fibre optic sensors, *Smart Materials and Structures*, vol. 10, no. 3, pp. 490-496, 2001.
- [2] P. Bettini, G. Sala, L. Di Landro and E. Tessadori, Embedded fibre optic techniques for primary structural components: strain and temperature monitoring, in European Conference on Composite Materials, Venice (Italy), 2012.
- [3] K. V. Grattan and T. Sun, Fiber optic sensor technology: an overview, *Sensors and Actuators A: Physical*, vol. 82, no. 1-3, pp. 40-61, 2000.
- [4] K. O. Hill and G. Meltz, Fiber Bragg grating technology fundamentals and overview, *Journal of lightwave technology*, vol. 15, no. 8, pp. 1263-1276, 1997.
- [5] G. Shaorui, J. Canning and K. Cook, Ultra-high temperature chirped fiber Bragg gratings produced by gradient stretching of viscoelastic silica, *Optics Letters*, vol. 38, no. 24, pp. 5397-5400, 2013.
- [6] T. Elsmann, A. Lorenz, N. S. Yazd, T. Habisreuther, J. Dellith, A. Schwuchow, J. Bierlich, K. Schuster, M. Rothhardt, L. Kido and H. Bartelt, High temperature sensing with fiber Bragg, *Optics Express*, vol. 22, no. 22, pp. 26825-26833, 2014.
- [7] J. Villatoro, A. Van Newkirk, E. Antonio-Lopez, J. Zubia, A. Schülzgen and R. Amezcua-Correa, Ultrasensitive vector bending sensor based on multicore optical fiber, *Optics Letters*, vol. 41, no. 4, pp. 832-835, 2016.
- [8] J. E. Antonio-Lopez, Z. Sanjabi Eznaveh, P. LiKamWa, A. Schülzgen and R. Amezcua-Correa, Multicore fiber sensor for high-temperature applications up to 1000°C, *Optics Letters*, vol. 39, no. 19, pp. 4309-4312, 2014.
- [9] A. Van Newkirk, Optimizacion of multicore fiber for high-temperature sensing *Optics Letters*, vol. 39, no. 16, 2014.